Chemical Science



EDGE ARTICLE

View Article Online
View Journal | View Issue



Cite this: Chem. Sci., 2024, 15, 17962

d All publication charges for this article have been paid for by the Royal Society of Chemistry

Received 3rd August 2024 Accepted 1st October 2024

DOI: 10.1039/d4sc05190d

rsc.li/chemical-science

Photocatalyst-free, visible-light-induced regioand stereoselective synthesis of phosphorylated enamines from *N*-allenamides *via* [1,3]-sulfonyl shift at room temperature†

Jia-Dong Guo,^a Feven-Alemu Korsaye, ^b Dorian Schutz, ^a Ilaria Ciofini ^b and Laurence Miesch ^a

Herein, we report the first visible-light-induced strategy for the rapid synthesis of densely functionalized α -and γ -phosphorylated β -sulfonyl enamines in a regio- and stereoselective manner from N-sulfonyl allenamides and H-phosphine oxides. The transformation displays a broad substrate scope, while operating at room temperature under photocatalyst- and additive-free conditions. In this atom-economical process, either terminal or substituted N-sulfonyl allenamides trigger an unprecedented N-to-C [1,3]-sulfonyl shift, relying on a dual radical allyl resonance and α -heteroatom effect in its triplet excited state. A plausible reaction mechanism is proposed which was supported by the outcomes of theoretical approaches based on Density Functional Theory (DFT) calculations.

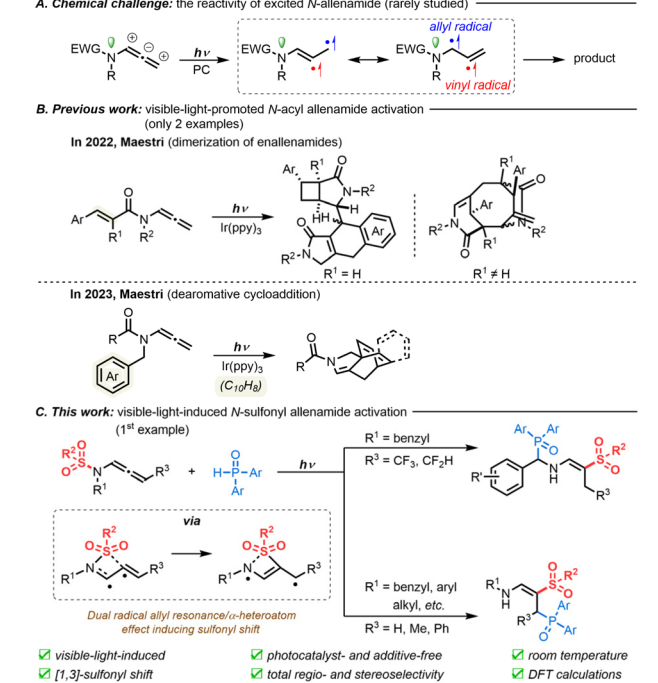
Introduction

The development of mild, efficient, and sustainable approaches to build complex molecular skeletons has become fundamental in organic synthesis today. Recent advancements in visible-light catalysis have made tremendous inroads toward these goals with the development of environmentally-friendly techniques. In this context, the activation of alkene functionalities allows the construction of complex molecular structures through either electron transfer or energy transfer from a species excited by visible-light irradiation. However, when it comes to allenes, visible-light catalysis remains highly challenging due to the formation of unstable vinyl radical species, whose unreliable reactivity can lead to various byproducts through unwanted reaction paths. 4

As readily available allene sources, *N*-allenamides bearing an electron-withdrawing group (EWG) on the nitrogen atom have emerged as powerful nitrogen-containing synthons in a variety of transformations.⁵ In contrast to their well-established

thermal reactivity, which depends on an electronic bias in their

ground state (S₀),6 their properties and reactivity in the triplet



 $\begin{tabular}{ll} Scheme 1 & Visible-light-induced activation of allenes in N-allenamide derivatives. \end{tabular}$

excited state (T₁) remain elusive (Scheme 1A). So far, only two examples, which involve a vinyl radical intramolecular addition

^eEquipe Synthèse Organique et Phytochimie, Institut de Chimie, CNRS-UdS, UMR 7177, 4 rue Blaise Pascal, CS 90032, 67081, Strasbourg, France. E-mail: lmiesch@unistra.fr

^bChemical Theory and Modelling Group, Chimie ParisTech, PSL University, CNRS, Institute of Chemistry for Life and Health Sciences, F-75005 Paris, France. E-mail: ilaria.ciofini@chimieparistech.psl.eu

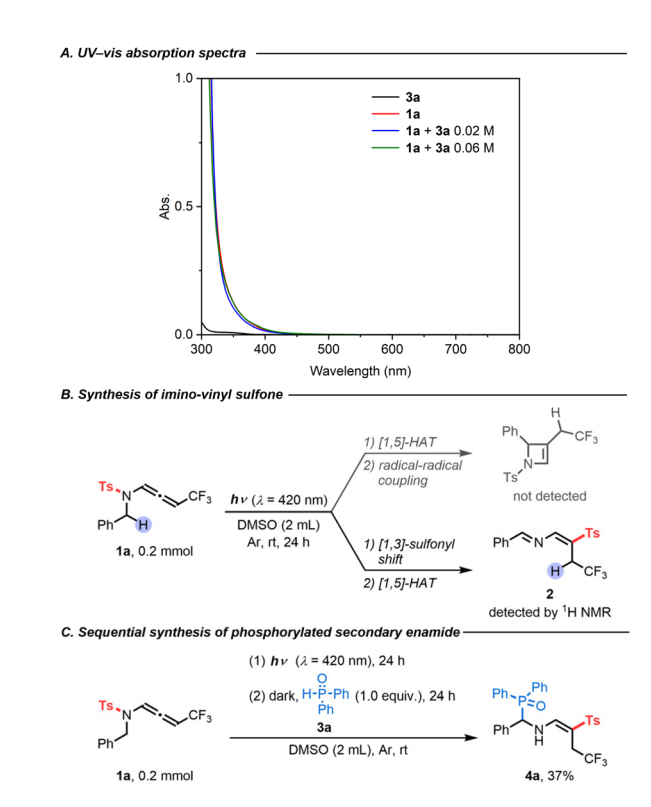
[†] Electronic supplementary information (ESI) available: Preparation of substrates, detailed optimization study, characterization of products, copies of NMR spectra, and computational details. CCDC 2281377, 2281378 and 2310786. For ESI and crystallographic data in CIF or other electronic format see DOI: https://doi.org/10.1039/d4sc05190d

process, have been depicted, using tailor-made N-acyl allenamides in the presence of an $Ir(ppy)_3$ photocatalyst (Scheme 1B). In 2022, Maestri's group reported the first visible-light-promoted dimerization of enallenamides to trigger a domino reaction for the synthesis of complex polycyclic systems. Later, the same group reported the preparation of complex [2.2.2]-(hetero)-bicyclooctadienes by the dearomative cycloaddition of N-acyl allenamides.

We were, however, puzzled that the reactivity of excited Nsulfonyl allenamides was still unexplored. We believed that the presence of the sulfonyl moiety could be used to our advantage to control the fate of the vinyl radical intermediate and to unlock new reactivities. We thus envisioned the following reaction design: Once a diradical species is formed, under visible-light, from N-allenamides, we reasoned that a direct Nto-C [1,3]-sulfonyl shift process could take place. Then, depending on the substrate pattern, two divergent pathways could be envisioned, yielding either α - or γ -phosphorylated β sulfonyl enamines following trapping by H-phosphine oxides. Such a strategy would provide densely functionalized compounds that incorporate relevant functional groups for drug discovery,9 including vinyl-sulfones10 and amino-phosphonates.11 In contrast to the numerous examples of N-S cleavage generating sulfonyl radicals through the use of radical initiators¹² or high-energy photons, ¹³ the direct N-to-C [1,3]sulfonyl shift of N-sulfonyl allenamides under visible-light irradiation would constitute a first, which could pave the way for unprecedented reactivity in the foreseeable future. Here, by using N-sulfonyl allenamides as substrates, we describe the first regio- and stereoselective synthesis of α - and γ -phosphorylated enamines in the presence of H-phosphine oxides under visiblelight irradiation (Scheme 1C).

Results and discussion

Initially, we tested our working hypothesis on CF₃-substituted N-allenamide 1a. As shown in its UV-visible absorption spectra, compound 1a exhibited a wide and strong absorption band in the UV-light region that slightly extends into the visible-light region ($\varepsilon = 0.45 \text{ L mol}^{-1} \text{ cm}^{-1} \text{ in 420 nm, Scheme 2A}$). At first, we envisioned that the highly reactive triplet state intermediate of compound 1a could potentially undergo a Norrish-Yang-type reaction,14 which would involve an intramolecular [1,5]hydrogen atom transfer (HAT)15 followed by radical-radical coupling to form an unsaturated azetidine (Scheme 2B).16 To test this hypothesis, we irradiated substrate 1a (0.2 mmol) in degassed DMSO (2 mL) with blue LEDs ($\lambda = 420$ nm) for 24 h at room temperature. However, the azetidine was not detected, while the formation of a new product - imino-vinyl sulfone 2 was observed by ¹H NMR (Scheme 2B). Such a product would result from a stereoselective N-to-C [1,3]-sulfonyl shift. Interestingly, the N-S bond dissociation energy of compound 1a, which was calculated to be 47.3 kcal mol⁻¹, ¹⁷ and the computed spin density distribution of the excited state as illustrated in the resonance forms (Scheme 1C) are consistent with a N-to-C [1,3]sulfonyl shift process.



Scheme 2 Preliminary experiments: (A) UV-vis absorption spectra of 3a (2.0 \times 10^{-2} M) in DMSO (black); 1a (2.0 \times 10^{-2} M) in DMSO (red); 1a (2.0 \times 10^{-2} M) and 3a (2.0 \times 10^{-2} M) in DMSO under an argon atmosphere (blue); 1a (2.0 \times 10^{-2} M) and 3a (6.0 \times 10^{-2} M) in DMSO under an argon atmosphere (green). (B) Synthesis of imino-vinyl sulfone. (C) Sequential synthesis of phosphorylated secondary enamide.

To facilitate the characterization of this compound, diphenylphosphine oxide (3a) was added to the reaction mixture after the photoreaction to engineer a carbo-phosphorylation, affording (E)-diphenyl(phenyl((4,4,4-trifluoro-2-tosylbut-1-en-1yl)amino)methyl)phosphine oxide (4a) in 37% yield (Scheme 2C).18 Furthermore, a direct addition of the H-phosphine oxide 3a to the CF₃-substituted N-sulfonyl allenamide 1a under visible-light irradiation ultimately produced the α-phosphorylated β-sulfonyl enamine 4a with a higher yield of 86% (Table 1, entry 1). Of note, no side products were observed in this atomeconomical process. During the optimization phase of this study, we screened a series of solvents, all of which showed lower reactivity but were still effective for the protocol (Table 1, entries 2-7). Moreover, the fact that the reaction does not proceed in the absence of visible-light irradiation supports the photoactivated nature of the reaction (Table S1,† entry 8). Anaerobic conditions were required for the transformation to take place (Table S1,† entry 9). Finally, a light on/off reaction was conducted (Fig. S7†), showing the advancement of transformation under blue LED irradiation. The absence of reaction in the dark is consistent with the necessity of a continuous irradiation.

Based on the above preliminary investigations, Density Functional Theory (DFT) and Time Dependent (TD-DFT)

Table 1 Variation from standard conditions ab

Entry	Solvent	Yield ^b (%)
1	None	86
2	MeCN	51
3	THF	28
4	Ethyl acetate	31
5	$\mathrm{CH_2Cl_2}$	32
6	Toluene	60
7	Acetone	14

^a Standard conditions: **1a** (0.2 mmol), **3a** (0.2 mmol, 1.0 equiv.) in DMSO (2 mL) was irradiated for 24 h with blue LEDs ($\lambda = 420$ nm) under an argon atmosphere at room temperature. ^b Isolated yields, n.r. = no reaction.

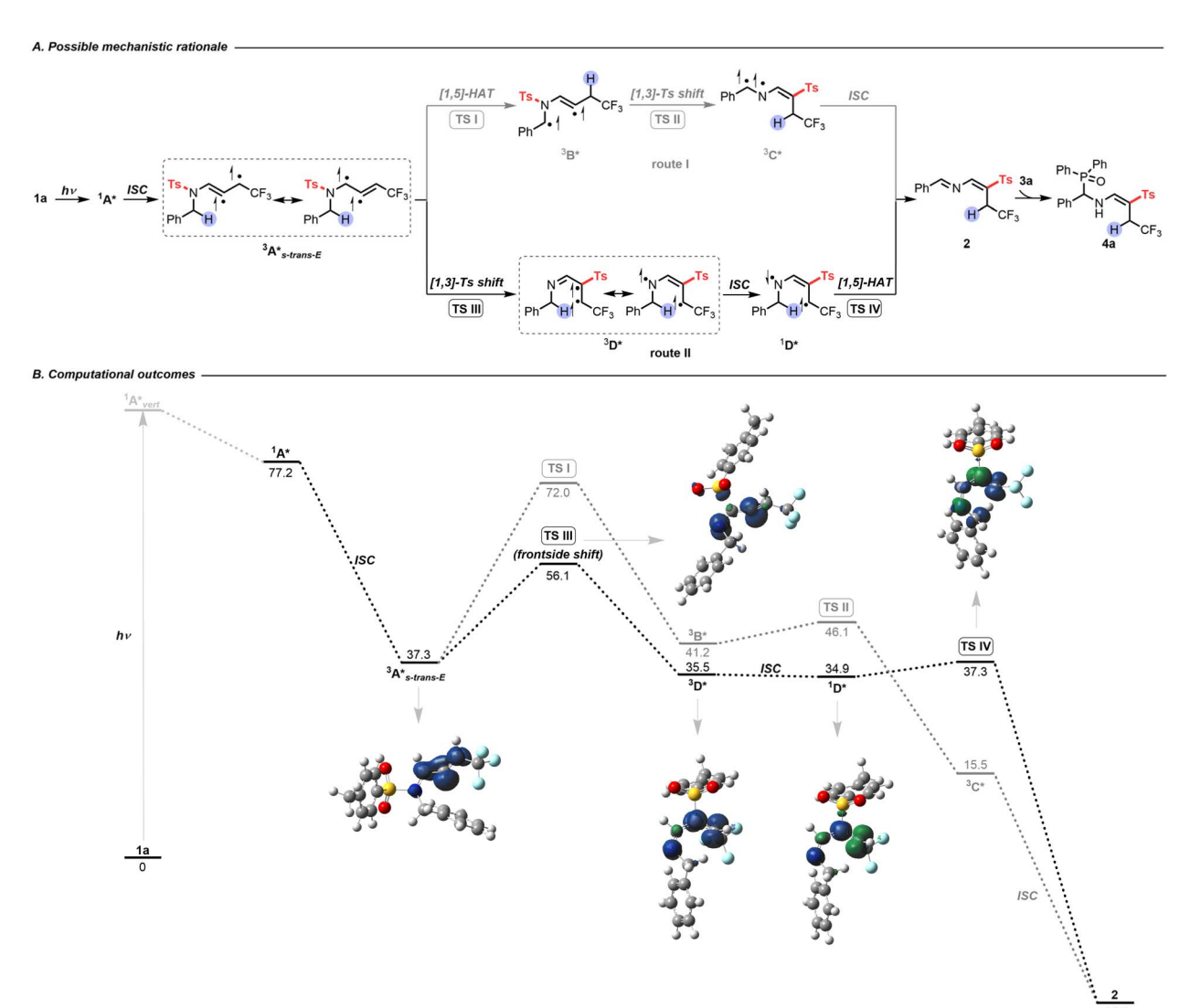
calculations suggested a possible mechanistic rationale as shown in Scheme 3. Under visible-light irradiation, compound 1a is promoted vertically to the intermediate ¹A*_{vert}, which undergoes vibrational relaxation to produce intermediate ¹A* (Fig. S3†). Subsequently, a triplet excited state diradical intermediate ³A* is generated through intersystem crossing (ISC) (Fig. S5†).19 To evaluate the most plausible geometry of intermediate ³A*, four possible conformations have been hypothesized. The intermediate ${}^{3}A^{*}_{s-trans-E}$ is found to be the most energetically stable and is therefore the one considered in the following study (Scheme S10†). At this point, two potential routes could exist: [1,5]-HAT followed by a [1,3]-tosyl (Ts) shift (route I, Scheme 3A); or [1,3]-Ts shift and subsequent [1,5]-HAT (route II, Scheme 3A). Comparing the Gibbs free energy of transition states **TS I** with **TS III**, a difference of 15.9 kcal mol⁻¹ is found, suggesting that route I is thermodynamically unfavorable. The triplet state intermediate ³D* is also found to be more energetically stable than intermediate ³B*, with a difference in Gibbs energy of 5.7 kcal mol⁻¹ (Scheme 3B). Route II involves a direct N-to-C [1,3]-Ts shift. A frontside or a backside shift of the Ts group on intermediate ³A* could take place to form the E or Z isomer of the diradical triplet intermediate ${}^{3}D^{*}$ (Scheme S11A†). The reaction mechanism for both isomers has thus been computed and is detailed in the ESI Scheme S11B.† These results show that the *E* isomer of all of the intermediates and transition states is more stable than the corresponding Zisomer, contributing to a total stereoselectivity for the *E* isomer. The intermediate ³**D*** could relax *via* ISC to give the singlet state diradical intermediate ${}^{1}D^{*}$, and a subsequent C-to-C [1,5]-HAT proceeds via transition state TS IV to produce imino-vinyl sulfone 2. For the latter step, radical-radical coupling for the intermediate ¹D* was ruled out as a competent mechanism, since it would either lead to the formation of a 4-membered ring with high strain, or, in the case of intramolecular radicalradical coupling, it was expected to be disfavoured with respect to the intramolecular H-transfer reaction that occurs practically spontaneously (with a barrier computed to be roughly 3.0 kcal

mol⁻¹). The energy profile indicates route II to be the most thermodynamically and kinetically favorable pathway. As no shift in the UV-visible absorption spectra of the reaction mixture in DMSO was detected, the photoactive electron donoracceptor (EDA) complex between 1a and 3a was negligible (Scheme 2A). Finally, quenching of imino-vinyl sulfone 2 with H-phosphine oxide 3a yields the amino-phosphinoyl alkene 4a, which is further functionalized with a tosyl sulfone.

With an understanding of the reaction mechanism, the viability of the visible-light-induced strategy was explored (Table 2). We examined a series of benzyl groups with different electron-donating groups (EDGs) and EWGs at various positions of the aromatic rings. Substituents at the para-position as well as at the ortho-position were tolerated, forming the corresponding products (4b-4l) in 68-95% yields. Moreover, substrate 1a was subjected to a scale-up reaction to demonstrate the practicality of the protocol, which provided a satisfactory yield of the target product 4a. X-ray analyses of 4l confirmed the structure of the α phosphorylated β-sulfonyl enamine (CCDC 2281377 contains the supplementary crystallographic data for the structure, see details in the ESI†).20 Disubstituted benzyl-groups (4m-4o) were also compatible with similar efficiency. Additionally, diversification of the process was demonstrated by carrying out the reaction in methanol (2 mL), leading to regio- and stereoselective formation of the corresponding alkoxy-amine 4p in 95% yield. The naphthyl derivative led to the desired product 4q in moderate yield. More interestingly, difluorinated N-allenamide 1r was used in this process, providing an interesting druglike enamine 4r.21 Decomposition of non-benzylic N-allenamide (1s) was observed under the reaction conditions because the formation of an imine moiety is excluded in this case (Scheme S4†).

We next focused on the scope of this transformation, using substrates encompassing different sulfonyl amides, including fluorinated sulfonyl groups (1t and 1u), as well as naphthyl (1v), alkyl (1w), and cycloalkyl (1x) derivatives, all of which reacted successfully to provide the corresponding α -phosphorylated β -sulfonyl enamines in high yields. Even thienyl derivatives proved suitable substrates, affording the corresponding product 4y in 87% yield. It was also possible to modify the H-phosphine oxides in this transformation. An array of H-phosphine oxides substituted with different EDGs and EWGs were tested, demonstrating their ability to provide the corresponding phosphorylated enamines (4z-4ad). The naphthyl derivative is also a viable compound, producing carbo-phosphorylated compound 4ae in 42% yield.

To highlight the sustainability of this synthetic process, we performed this reaction under sunlight irradiation for two days. In this way, the target phosphorylated enamine was obtained in 77% yield. Furthermore, imino-vinyl sulfone 2 was efficiently reduced by $\rm Et_3SiH$ and $\rm BF_3 \cdot Et_2O$, producing secondary enamine 5 in 82% yield. X-ray analyses of 5 confirmed its structure, and facilitated the assignment of the stereochemistry of the double bond (CCDC 2281378 contains the supplementary crystallographic data for the structure, see details in the ESI†). In addition, hydrolysis of the imine



Scheme 3 (A) Possible mechanistic rationale. (B) Computational outcomes. Gibbs free energies (kcal mol^{-1}) were computed at the PBE0/6-311++G(d,p) level of theory using DMSO as an implicit solvent with the PCM method. Spin densities are reported for the triplet and singlet diradical states (isocontour value 0.01 au).

intermediate under basic conditions provided primary enamine ${\bf 6}$ in 53% yield. 25

After developing an interest in the visible-light-induced N-to-C [1,3]-sulfonyl shift, we wondered whether this strategy could be expanded beyond CF₃-substituted N-allenamides. Upon employing terminal N-allenamides in the presence of H-phosphine oxides, we observed a different outcome, resulting in a completely different hydrophosphorylated product. It is noteworthy that the nature of the phosphorylated product changes based simply on the substitution pattern of the substrates. In this case, we hypothesized that an intermolecular HAT takes place followed by addition of a phosphinoyl radical $[P(O)\cdot]$ to the terminal part of the alkene, affording γ -phosphorylated β -sulfonyl enamines 8 (Scheme 4A). As no spectral shift of the reaction mixture in DMSO could be detected in the UV-visible absorption spectra, formation of a photoactive EDA complex between 7a and 3a seems unlikely (Fig. S2†). In the

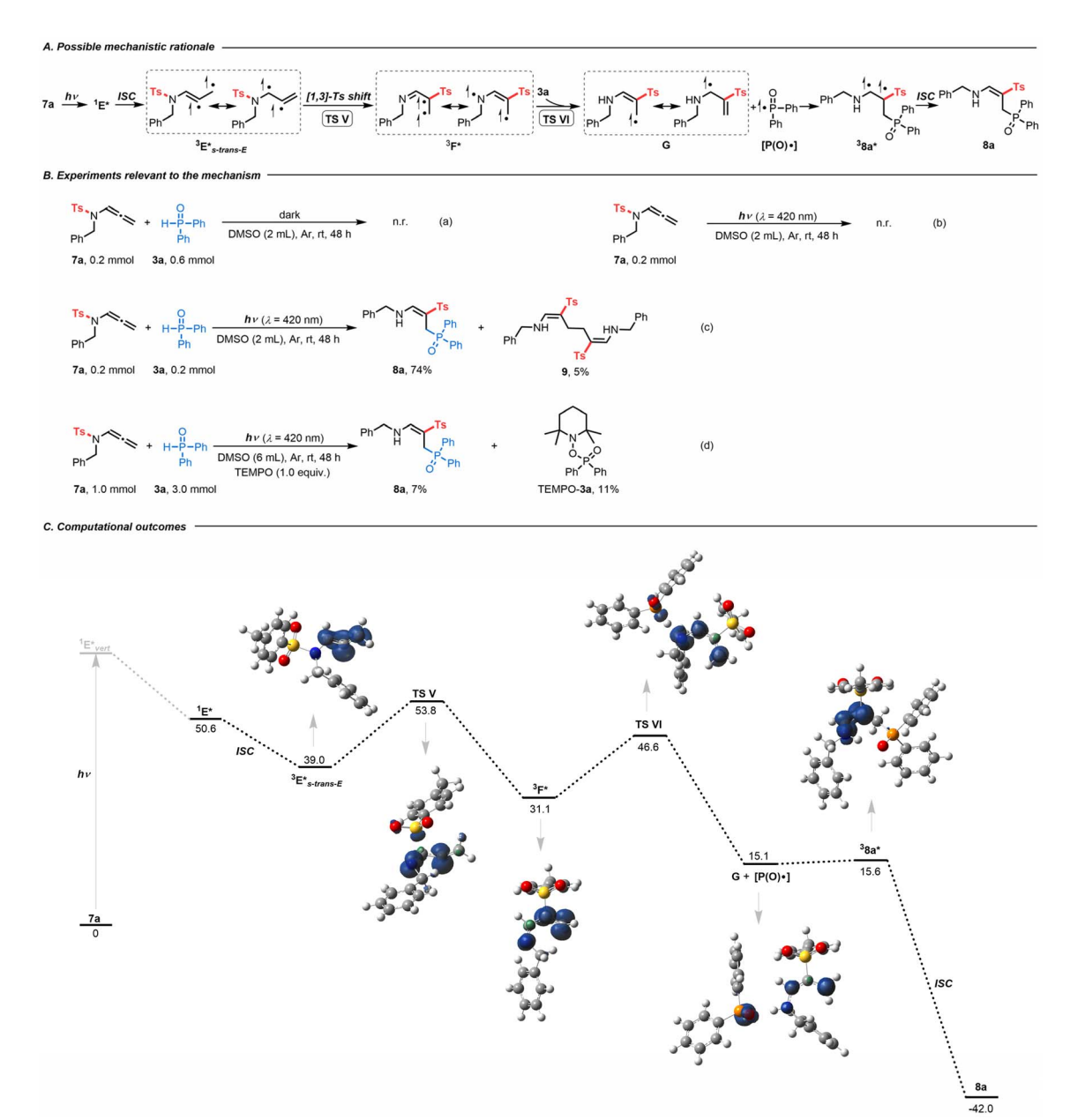
absence of light irradiation, no reaction took place, which proved its photocatalytic nature [Scheme 4B(a)]. Control experiments suggested the necessity of a hydrogen atom donor. When we carried out the reaction without H-phosphine oxide 3a, starting material 7a was completely recovered, which might be attributed to the diminished reactivity of the allylic radical [Scheme 4B(b)]. With the addition of starting materials 7a (0.2) mmol, 1.0 equiv.) and 3a (1.0 equiv.) in degassed DMSO (2 mL) and irradiation for 48 h at room temperature, the homodimerization compound 9 was obtained in 5% yield, providing evidence for the formation of transient terminal allyl radical G [Scheme 4B(c)].26 The radical inhibitor 2,2,6,6-tetramethylpiperidin-1-oxyl (TEMPO) greatly suppressed the reaction, with 8a formed in only about 7% yield. Importantly, compound TEMPO-3a was detected by ¹H NMR, supporting the generation of phosphinoyl radicals $[P(O) \cdot]$ (Scheme 4B(d)).

Table 2 Substrate scope of α-phosphorylated β-sulfonyl enamines abcd

DFT calculations provided more details on the regioselective phosphorylation (Scheme 4C). With visible-light irradiation, 7a is promoted vertically to intermediate ${}^{1}E^{*}_{vert}$, which undergoes vibrational relaxation to produce intermediate ${}^{1}E^{*}$ (Fig. S4†). Through ISC, the triplet diradical intermediate ${}^{3}E^{*}$ can be

formed (Fig. S6†). At this point a stereoselective frontside N-to-C [1,3]-Ts shift (**TS V**) occurs to form intermediate ${}^3\mathbf{F}^*$. In this case H-phosphine oxide demonstrated its utility as a hydrogen atom donor, facilitating the formation of intermediate **G** and phosphinoyl radical [$P(O) \cdot]$ *via* transition state **TS VI**.²⁷ Radical allylic

^a Reaction condition A: 1 (0.2 mmol), 3 (0.2 mmol, 1.0 equiv.) in DMSO (2 mL) was irradiated for 24 h with blue LEDs ($\lambda=420$ nm) under an argon atmosphere at room temperature. ^b Isolated yields. ^c Scale-up reaction: 1a (2.5 mmol), 3a (2.5 mmol, 1.0 equiv.) in DMSO (15 mL) was irradiated for 24 h with blue LEDs ($\lambda=420$ nm) under an argon atmosphere at room temperature. ^d Reaction condition B: 1a (0.2 mmol) in MeOH (2 mL) was irradiated for 24 h with blue LEDs ($\lambda=420$ nm) under an argon atmosphere at room temperature.



Scheme 4 (A) Possible mechanistic rationale. (B) Experiments relevant to the mechanism. (C) Computational outcomes. Gibbs free energies (kcal mol^{-1}) computed at the PBE0/6-311++G(d,p) level of theory using DMSO as an implicit solvent with the PCM method. Spin densities are reported for the triplet and singlet diradical states (isocontour value 0.01 au).

resonance enables the addition of the phosphinoyl radical $[P(O)\cdot]$ to the terminal alkene, affording triplet diradical intermediate ${}^38a^*$. Finally, ISC led to the formation of γ -phosphorylated β -sulfonyl enamine 8a.

We then explored the generality of this reaction. Under reaction condition C (Table 3), different benzyl-substituted terminal N-sulfonyl allenamides showed high reactivity to form the corresponding products (8a–8e) with complete control of regio- and stereoselectivity. X-Ray analyses of 8a confirmed the structure of the γ -phosphorylated β -sulfonyl enamine (CCDC 2310786 contains the supplementary crystallographic data for the structure, see details in the ESI†). Scale-up reactions led to 8a with a slight erosion of the yield (81 ν s. 65%). Importantly,

this protocol was also compatible with thienyl-substituted substrates producing **8f** in 62% yield. Phenyl moieties on the nitrogen atom were utilized to generate desired products (**8g-8j**) in 70–80% yields. Linear alkyls (7**k**) and cyclopropyls (7**l**) proved compatible, allowing the formation of the corresponding phosphorylated enamines in 47 and 73%, respectively. The delocalization of spin densities may explain the preservation of the *N*-cyclopropyl arm of product **8l**, with the rate of ring-opening of an α -cyclopropyl radical typically being inversely proportional to the degree of spin delocalization of the nucleus. ²⁹ Additionally, functionalized side chains (7**m**, 7**n** and 7**o**) underwent a [1,3]-Ts shift, expanding the chemical space of those structures. Terminal *N*-sulfonyl allenamides with

Table 3 Substrate scope of γ -phosphorylated β-sulfonyl enamines abcd

different aryl ($7\mathbf{p}$) and heteroaryl ($7\mathbf{q}$) sulfonyls on the nitrogen atom, were also effective for this *N*-to-*C* [1,3]-sulfonyl shift reaction. In addition, H-phosphine oxides substituted with 4-^tBu- and 3,5-Me- were converted to the corresponding products 8**r** and 8**s** in 88 and 84% yields, respectively.

Conceivably, the outcome of the transformation is closely related to the stability of the allylic radical involved. Similar to terminal N-allenamides, the Me-N-allenamide 7t led to the formation of γ -phosphorylated β -sulfonyl enamine 8t. Benzylic allylic radicals generated through photoactivation of Ph-N-allenamide 7u followed the same trend, yielding the corresponding γ -phosphorylated β -sulfonyl enamine 8u. In contrast, the presence of -CF $_3$ or -CF $_2$ H stabilizes the allylic radical, hence favoring the intramolecular [1,5]-HAT process providing α -phosphorylated β -sulfonyl enamines. Some limitations of the method were also observed, for example, phenol and thiophenol did not lead to formation of the corresponding products 8v and 8w.

Conclusions

We report herein the first visible-light-induced strategy for the synthesis of α - and γ -phosphorylated β -sulfonyl enamines from *N*-sulfonyl allenamides in the presence of H-phosphine oxides under catalyst- and additive-free conditions. This simple,

efficient, and atom-economical process exhibits a broad substrate scope, excellent functional compatibility and complete regio- and stereo-selectivity. In addition, a scale-up reaction and sunlight irradiation make the developed method sustainable and amenable for potentially operational procedures. We anticipate that the unique mechanistic features discovered here, involving the high reactivity of excited *N*-allenamides, will have broad implications beyond this work.

Data availability

All data presented in this manuscript are available in the ESI.†

Author contributions

L. M. and J.-D. G. conceived and designed the experiments. L. M. directed the project. J.-D. G and D. S. performed the experiments. F.-A. K. performed the DFT calculations. I. C. supervised the theoretical work. L. M., J.-D. G., I. C. and F.-A. K. wrote the paper. L. M., J.-D. G., I. C., F.-A. K. and D. S. discussed the results and commented on the manuscript.

Conflicts of interest

The authors declare no conflict of interest.

^a Reaction condition C: 7 (0.2 mmol), 3 (0.6 mmol, 3.0 equiv.) in DMSO (2 mL) was irradiated for 48 h with blue LEDs ($\lambda = 420$ nm) under an argon atmosphere at room temperature. ^b Isolated yields. ^c Scale-up reaction: 7a (2.5 mmol), 3a (2.5 mmol, 1.0 equiv.) in DMSO (15.0 mL) was irradiated for 48 h with blue LEDs ($\lambda = 420$ nm) under an argon atmosphere at room temperature. ^d 72 h.

Acknowledgements

The authors wish to thank Prof. L. Ruhlmann, Dr J. Sun, Dr J. Massue and Dr V. Lebrun for fruitful discussions about the photophysical properties of *N*-allenamides. J.-D. Guo. thanks the International Center for Frontier Research in Chemistry (icFRC)-Fondation Jean-Marie LEHN for a post-doctoral fellowship.

References

Edge Article

- (a) G. E. M. Crisenza and P. Melchiorre, *Nat. Commun.*, 2020,
 11, 803; (b) M. Tavakolian, S. Vahdati-Khajeh and S. Asgari, *ChemCatChem*, 2019, 11, 2943; (c) C. Wang, X. Chen, M. Qi,
 J. Wu, G. Gözaydın, N. Yan, H. Zhong and F. Jin, *Green Chem.*, 2019, 21, 6089.
- 2 (a) S.-L. Meng, C. Ye, X.-B. Li, C.-H. Tung and L.-Z. Wu, J. Am. Chem. Soc., 2022, 144, 16219; (b) M. Sayed, J. Yu, G. Liu and M. Jaroniec, Chem. Rev., 2022, 122, 10484; (c) A. Y. Chan, I. B. Perry, N. B. Bissonnette, B. F. Buksh, G. A. Edwards, L. I. Frye, O. L. Garry, M. N. Lavagnino, B. X. Li, Y. Liang, E. Mao, A. Millet, J. V. Oakley, N. L. Reed, H. A. Sakai, C. P. Seath and D. W. C. MacMillan, Chem. Rev., 2022, 122, 1485; (d) P. R. D. Murray, J. H. Cox, N. D. Chiappini, C. B. Roos, E. A. McLoughlin, B. G. Hejna, S. T. Nguyen, H. H. Ripberger, J. M. Ganley, E. Tsui, N. Y. Shin, B. Koronkiewicz, G. Qiu and R. R. Knowles, Chem. Rev., 2022, 122, 2017; (e) N. Hammer, M. L. Christensen, Y. Chen, D. Naharro, F. Liu, K. A. Jorgensen and K. N. Houk, J. Am. Chem. Soc., 2020, 142, 6030; (f) D. A. Nicewicz and D. W. C. MacMillan, Science, 2008, 322, 77.
- 3 (a) J. Großkopf, T. Kratz, T. Rigotti and T. Bach, *Chem. Rev.*, 2022, **122**, 1626; (b) S. O. Badir and G. A. Molander, *Chem*, 2020, **6**, 1327.
- 4 (*a*) J. Singh, A. Sharma and A. Sharma, *Org. Chem. Front.*, 2021, **8**, 5651; (*b*) A. B. Rolka and B. Koenig, *Org. Lett.*, 2020, **22**, 5035; (*c*) N. Arai and T. Ohkuma, *Org. Lett.*, 2019, **21**, 1506.
- 5 (a) C. Gommenginger, Y. Zheng, D. Maccarone, I. Ciofini and L. Miesch, Org. Chem. Front., 2023, 10, 4055; (b) M. Hourtoule and L. Miesch, Org. Lett., 2023, 25, 1727; (c) M. Hourtoule and L. Miesch, Org. Biomol. Chem., 2022, 20, 9069; (d) Y. Zheng, B. Moegle, S. Ghosh, A. Perfetto, D. Luise, I. Ciofini and L. Miesch, Chem.-Eur. J., 2022, 28, e202103598; (e) X. Li, Y. Liu, N. Ding, X. Tan and Z. Zhao, RSC Adv., 2020, 10, 36818; (f) T. Lu, Z. Lu, Z.-X. Ma, Y. Zhang and R. P. Hsung, Chem. Rev., 2013, 113, 4862; (g) L.-L. Wei, H. Xiong and R. P. Hsung, Acc. Chem. Res., 2003, 36, 773.
- 6 (a) X. Zhong, J. Tan, J. Qiao, Y. Zhou, C. Lv, Z. Su, S. Dong and X. Feng, Chem. Sci., 2021, 12, 9991; (b) Y. Wang, P. Zhang, X. Di, Q. Dai, Z.-M. Zhang and J. Zhang, Angew. Chem., Int. Ed., 2017, 56, 15905; (c) Y. Ning, Q. Ji, P. Liao, E. A. Anderson and X. Bi, Angew. Chem., Int. Ed., 2017, 56, 13805; (d) R.-R. Liu, J.-P. Hu, J.-J. Hong, C.-J. Lu, J.-R. Gao and Y.-X. Jia, Chem. Sci., 2017, 8, 2811.

- 7 A. Serafino, M. Chiminelli, D. Balestri, L. Marchiò, F. Bigi, R. Maggi, M. Malacria and G. Maestri, *Chem. Sci.*, 2022, 13, 2632.
- 8 M. Chiminelli, A. Serafino, D. Ruggeri, L. Marchiò, F. Bigi, R. Maggi, M. Malacria and G. Maestri, *Angew. Chem., Int. Ed.*, 2023, **62**, e202216817.
- 9 C. Castiello, P. Junghanns, A. Mergel, C. Jacob, C. Ducho, S. Valente, D. Rotili, R. Fioravanti, C. Zwergel and A. Mai, *Green Chem.*, 2023, 25, 2109.
- 10 (a) X. Yu, Z. Zhang and G. Dong, J. Am. Chem. Soc., 2022, 144, 9222; (b) R. Ahmadi and S. Emami, Eur. J. Med. Chem., 2022, 234, 114255; (c) M. N. Noshi, A. El-awa, E. Torres and P. L. Fuchs, J. Am. Chem. Soc., 2007, 129, 11242; (d) B. A. Frankel, M. Bentley, R. G. Kruger and D. G. McCafferty, J. Am. Chem. Soc., 2004, 126, 3404.
- 11 (a) A. Maestro, X. del Corte, A. López-Francés, E. Martínez de Marigorta, F. Palacios and J. Vicario, Molecules, 2021, 26, 3202; (b) V. Quint, N. Chouchène, M. Askri, J. Lalevée, A.-C. Gaumont and S. Lakhdar, Org. Chem. Front., 2019, 6, 41; (c) W.-Q. Liu, T. Lei, S. Zhou, X.-L. Yang, J. Li, B. Chen, J. Sivaguru, C.-H. Tung and L.-Z. Wu, J. Am. Chem. Soc., 2019, 141, 13941; (d) S. Martić and H.-B. Kraatz, Chem. Sci., 2013, 4, 42.
- 12 B.-C. Wang, T. Fan, F.-Y. Xiong, P. Chen, K.-X. Fang, Y. Tan, L.-Q. Lu and W.-J. Xiao, *J. Am. Chem. Soc.*, 2022, **144**, 19932.
- (a) P.-P. Yeh, J. E. Taylor, D. G. Stark, D. S. B. Daniels,
 C. Fallan, J. C. Walton and A. D. Smith, *Org. Biomol. Chem.*, 2017, 15, 8914; (b) F. W. Stacey, J. C. Sauer and
 B. C. McKusick, *J. Am. Chem. Soc.*, 1959, 81, 987.
- 14 (a) S. Majhi, Photochem. Photobiol. Sci., 2021, 20, 1357; (b)
 C. Chen, Org. Biomol. Chem., 2016, 14, 8641; (c) N. C. Yang and D.-D. H. Yang, J. Am. Chem. Soc., 1958, 80, 2913; (d)
 R. G. W. Norrish, Trans. Faraday Soc., 1937, 33, 1521.
- (a) W. Guo, Q. Wang and J. Zhu, Chem. Soc. Rev., 2021, 50, 7359;
 (b) S. A. Green, S. W. M. Crossley, J. L. M. Matos, S. Vásquez-Céspedes, S. L. Shevick and R. A. Shenvi, Acc. Chem. Res., 2018, 51, 2628.
- 16 (a) M. J. Oddy, D. A. Kusza, R. G. Epton, J. M. Lynam, W. P. Unsworth and W. F. Petersen, *Angew. Chem., Int. Ed.*, 2022, 61, e202213086; (b) A. D. Richardson, M. R. Becker and C. S. Schindler, *Chem. Sci.*, 2020, 11, 7553.
- 17 Y.-R. Luo, Comprehensive Handbook of Chemical Bond Energies, CRC Press, Boca Raton, FL, 1st edn, 2007.
- 18 (a) K. Ogura, I. Isozumi, T. Takehara, T. Suzuki and S. Nakamura, Org. Lett., 2022, 24, 8088; (b) N. Popovics-Tóth, T. D. T. Bao, Á. Tajti, B. Mátravölgyi, Z. Kelemen, F. Perdih, L. Hackler, L. G. Puskás and E. Bálint, ACS Omega, 2022, 8, 2698; (c) T. Xiong, X. Zhou and J. Jiang, Org. Biomol. Chem., 2022, 20, 5721; (d) Q. Huang, L. Zhu, D. Yi, X. Zhao and W. Wei, Chin. Chem. Lett., 2020, 31, 373.
- 19 (a) J.-D. Guo, Y.-J. Chen, C.-H. Wang, Q. He, X.-L. Yang, T.-Y. Ding, K. Zhang, R.-N. Ci, B. Chen, C.-H. Tung and L.-Z. Wu, Angew. Chem., Int. Ed., 2023, 62, e202214944; (b)
 T. J. Penfold, E. Gindensperger, C. Daniel and C. M. Marian, Chem. Rev., 2018, 118, 6975; (c) T. Itoh, Chem. Rev., 2012, 112, 4541.

20 CCDC 2281377 (4I) contains the supplementary crystallographic data for this paper. These data can be obtained free of charge from the Cambridge Crystallographic Data Centre.†

Chemical Science

- 21 (a) J. Majhi, R. K. Dhungana, A. Rentería-Gómez, M. Sharique, L. Li, W. Dong, O. Gutierrez and G. A. Molander, J. Am. Chem. Soc., 2022, 144, 15871; (b) J. Wang, M. Sánchez-Roselló, J. L. Aceña, C. del Pozo, A. E. Sorochinsky, S. Fustero, V. A. Soloshonok and H. Liu, Chem. Rev., 2014, 114, 2432; (c) N. A. Meanwell, J. Med. Chem., 2011, 54, 2529.
- 22 (a) J.-D. Guo, X.-L. Yang, B. Chen, C.-H. Tung and L.-Z. Wu, *Green Chem.*, 2021, 23, 7193; (b) R. A. Sheldon, *ACS Sustain. Chem. Eng.*, 2018, 6, 32.
- 23 P.-F. Zheng, Q. Ouyang, S.-L. Niu, L. Shuai, Y. Yuan, K. Jiang, T.-Y. Liu and Y.-C. Chen, J. Am. Chem. Soc., 2015, 137, 9390.
- 24 CCDC 2281378 (5) contains the supplementary crystallographic data for this paper. These data can be obtained free of charge from the Cambridge Crystallographic Data Centre.†
- 25 (a) R. R. Aleti, A. A. Festa, O. A. Storozhenko, V. L. Bondarev, O. O. Segida, S. A. Paveliev, V. B. Rybakov, A. V. Varlamov and

- L. G. Voskressensky, *Org. Lett.*, 2022, **24**, 9337; (*b*) L. Martínez-Montero, A. Díaz-Rodríguez, V. Gotor, V. Gotor-Fernández and I. Lavandera, *Green Chem.*, 2015, **17**, 2794; (*c*) G. Fernández de Trocóniz, A. M. Ochoa de Retana, S. Pascual, J. M. Ezpeleta and F. Palacios, *Eur. J. Org Chem.*, 2013, **2013**, 5614.
- 26 D. Leifert and A. Studer, *Angew. Chem., Int. Ed.*, 2020, 59, 74.
 27 (a) H. Ren, P. Zhang, J. Xu, W. Ma, D. Tu, C. S. Lu and H. Yan, *J. Am. Chem. Soc.*, 2023, 145, 7638; (b) J. Li, Z. Zhang, L. Wu, W. Zhang, P. Chen, Z. Lin and G. Liu, *Nature*, 2019, 574, 516.
- 28 CCDC 2310786 (8a) contains the supplementary crystallographic data for this paper. These data can be obtained free of charge from the Cambridge Crystallographic Data Centre.†
- (a) N. Genossar, P. B. Changala, B. Gans, J. C. Loison,
 S. Hartweg, M. A. Martin-Drumel, G. A. Garcia,
 J. F. Stanton, B. Ruscic and J. H. Baraban, *J. Am. Chem. Soc.*, 2022, 144, 18518; (b) X. Guan and D. L. Phillips,
 THEOCHEM, 2007, 811, 135; (c) J. H. Horner, N. Tanaka
 and M. Newcomb, *J. Am. Chem. Soc.*, 1998, 120, 10379.